

Intercomparison of tropospheric ozone models: Ozone transport in a complex tropopause folding event

G. J. Roelofs,¹ A. S. Kentarchos,^{1,2} T. Trickl,³ A. Stohl,⁴ W. J. Collins,⁵ R. A. Crowther,⁶ D. Hauglustaine,⁷ A. Klonecki,⁷ K. S. Law,⁶ M. G. Lawrence,⁸ R. von Kuhlmann,⁸ and M. van Weele⁹

Received 29 January 2003; revised 23 April 2003; accepted 2 May 2003; published 18 June 2003.

[1] The present generation of tropospheric chemistry models applies horizontal and vertical model resolutions that are sufficiently fine to represent synoptic-scale processes. In this study we compare simulations of a tropopause folding event on 20–21 June 2001 from six tropospheric ozone models with tropospheric ozone profiles observed at Garmisch-Partenkirchen (Germany). The event involves air masses of stratospheric origin and of North Atlantic and North American tropospheric origin. Two coupled chemistry-climate models, three chemistry-transport models, and one chemistry-trajectory model participate in the intercomparison. The models do not explicitly include stratospheric chemistry, and stratospheric ozone is parameterized instead. The horizontal resolution of the Eulerian models, T42 ($2.8^\circ \times 2.8^\circ$) or finer, appears adequate to represent two prominent features, namely, the stratospheric intrusion descending from the upper troposphere to about 4 km altitude on the first day and an ozone-poor air mass of marine origin in the lower troposphere on the second day. The ozone distribution from the Lagrangian model is less representative because of an insufficient air parcel density. Major discrepancies between model results and observations are the underestimation of ozone levels in the intrusion, too strong downward transport of ozone between the lower stratosphere and the upper troposphere on the first day, and too fast and deep descent of the intrusion. Accurate representation of ozone levels in the intrusion depends directly on the accuracy of the simulated ozone in the lower stratosphere. Additionally, for Eulerian models a relatively coarse vertical resolution in the tropopause region may add to inaccuracies in the simulated ozone distributions.

INDEX TERMS: 0322 Atmospheric Composition and Structure: Constituent sources and sinks; 0365 Atmospheric Composition and Structure: Troposphere—composition and chemistry; 0368 Atmospheric Composition and Structure: Troposphere—constituent transport and chemistry; 3362 Meteorology and Atmospheric Dynamics: Stratosphere/troposphere interactions; *KEYWORDS:* tropospheric ozone, stratosphere-troposphere exchange, numerical modeling

Citation: Roelofs, G. J., et al., Intercomparison of tropospheric ozone models: Ozone transport in a complex tropopause folding event, *J. Geophys. Res.*, 108(D12), 8529, doi:10.1029/2003JD003462, 2003.

1. Introduction

[2] Tropospheric ozone is an important trace gas in atmospheric chemistry and climate studies because it deter-

mines the oxidation capacity of the atmosphere through photodissociation and subsequent reaction of $O(^1D)$ with water vapor to produce OH radicals [Levy, 1971], and it is a greenhouse gas [Ramanathan et al., 1987]. Ozone is photochemically produced as a byproduct of the oxidation of hydrocarbons emitted by natural and anthropogenic processes. Anthropogenic activities have caused a tropospheric ozone increase relative to the pre-industrial atmosphere [Lelieveld et al., 1999]. The anthropogenic contribution can only be determined accurately if the strength of natural tropospheric ozone sources is known. Stratosphere-troposphere exchange (STE), which is a natural source, transports relatively ozone-rich air from the stratosphere into the troposphere. Model estimates of the global annual cross-tropopause ozone flux range between 400 and 1400 Tg O_3 year⁻¹ [Prather et al., 2001].

[3] STE occurs mostly in tropopause folds and cut-off lows, generated by baroclinic disturbances in the meandering jet stream associated with mesoscale convective

¹Institute for Marine and Atmospheric Research Utrecht, Utrecht University, Utrecht, Netherlands.

²Now at Environmental Research & Services, Florence, Italy.

³Institut für Meteorologie und Klimaforschung, Forschungszentrum Karlsruhe, Garmisch-Partenkirchen, Germany.

⁴Department of Ecology, Technical University Munich, Freising-Weihenstephan, Germany.

⁵Met Office, Bracknell, UK.

⁶Centre for Atmospheric Science, University of Cambridge, Cambridge, UK.

⁷Laboratoire des Sciences du Climat et de L'Environnement, Gif-sur-Yvette, France.

⁸Max Planck Institute for Chemistry, Mainz, Germany.

⁹Royal Netherlands Meteorological Institute, De Bilt, Netherlands.

complexes and thunderstorms [Holton *et al.*, 1995; Appenzeller *et al.*, 1996; Vaughan, 1988; Davies and Schüpbach, 1994]. Generally, synoptic disturbances involve transport of different air masses [e.g., Cooper *et al.*, 2001]. Part of the stratospheric air that is pulled downward into the troposphere in the trough of the tropopause fold mixes irreversibly into the troposphere. Simultaneously, lower tropospheric air masses ascend in warm and cold conveyor belts and are deposited in the upper and middle troposphere, respectively. Hence these disturbances are a mechanism for mixing stratospheric air into the troposphere and for intercontinental transport of pollutants. The latter is widely studied at present through campaigns such as NARE and MINOS, and through model studies (e.g., Fehsenfeld *et al.* [1996] (see also International Global Atmospheric Chemistry project (IGAC), IGACtivities, issue 24, 2001, at <http://www.igac.unh.edu>), Lelieveld *et al.* [2002], Stohl and Trickl [1999], Jacob *et al.* [1999], Roelofs *et al.* [2003], and Trickl *et al.* [2003]).

[4] The present generation of Eulerian 3-D atmospheric chemistry models often uses horizontal and vertical model resolutions that appear to be sufficient to represent synoptic-scale processes [e.g., Kentarchos *et al.*, 2000]. This study presents an intercomparison of tropospheric ozone models. It focuses on a tropopause folding event at extra-tropical latitudes and the associated transport between the stratosphere and the troposphere and within the troposphere. The study is part of the EU project STACCATO (Influence of Stratosphere-Troposphere Exchange in a Changing Climate on Atmospheric Transport and Oxidation Capacity). The aim of STACCATO was to develop a new three-dimensional perspective of STE, based on modeling activities and observations. Stohl *et al.* [2003] present an overview of STACCATO.

[5] Previous ozone model intercomparisons considered monthly, seasonal and annual tropospheric ozone distributions and budgets. Kanakidou *et al.* [1998] present an intercomparison of thirteen models. The models reproduced the seasonalities of observed monthly surface ozone, while discrepancies between observed and modeled concentrations at the surface were below 50%. Larger discrepancies were found in the free troposphere and in the tropopause region where transport processes dominate the ozone distribution. Law *et al.* [2000] compared simulated ozone in the upper troposphere (UT) and lower stratosphere (LS) from five models with an ozone climatology derived from MOZAIC (Measurement of Ozone and Water Vapor by Airbus In-Service Aircraft). The models generally showed good agreement with observations but often failed to capture sharp ozone concentration gradients in the tropopause region and between extra-tropical and tropical regions. A third intercomparison of ozone models focused on the seasonality of LS ozone and the role of vertical transport [Bregman *et al.*, 2001]. It was found that chemistry-transport models may simulate highly different vertical transport efficiencies in the LS, even when they apply meteorological data from the same source to calculate advection, e.g., from ECMWF analysis. The tracer transport schemes used in the models are of additional influence. We note that Meloen *et al.* [2003] and Cristofanelli *et al.* [2003] evaluate several models, including three from this study, by analyzing simulations of an STE event over Europe on 26

May 1996 in terms of vertical transport, idealized tracer distributions and ozone profiles. The study of Meloen *et al.* [2003] shows that simulated vertical velocities in the troposphere in and near an intrusion are fairly consistent between models.

[6] Section 2 presents the observed ozone profiles against which the simulation results are evaluated. An overview of all observational data associated with the same event is presented by Zanis *et al.* [2003]. The six tropospheric ozone models from European research institutes that participated in the intercomparison are presented in section 3. In section 4 we compare the model results and lidar profiles. Section 5 presents an analysis of the contribution of stratospheric ozone to tropospheric ozone levels during the event. We also examine the sensitivity of tropospheric ozone concentrations to stratospheric ozone abundances. In section 6 the results will be summarized and discussed.

2. Presentation of the Measurements

[7] Figure 1 shows vertical ozone profiles observed on 20 and 21 June 2001 at Garmisch-Partenkirchen (Germany, 47.5°N, 11.1°E). Ozone is measured with a differential absorption lidar (DIAL), installed at 740 m above MSL and operated at the wavelengths 277, 292 and 313 nm. It yields ozone profiles between 0.2 km above the ground and roughly 3 km above the tropopause, with a vertical resolution of 50 m in the lower troposphere and 500 m around the tropopause. The measurements have a time resolution of 2 hours. The accuracy for ozone is about 3 ppbv below 6 km altitude and about 5 ppbv between 6 km and the tropopause [Eisele *et al.*, 1999].

[8] The measurements commenced about one day after the onset of a tropopause folding event. A relatively ozone-rich air mass (80–120 ppbv) is clearly visible as a layer of ~2 km thickness, presumably of stratospheric origin. In the morning of 20 June it is located between 6 and 8 km altitude, and in the next 24 hours it descends gradually to about 3 km altitude. Air masses containing relatively low ozone levels are observed immediately after the intrusion, specifically on 20 June between 0800 and 2000 UT between 8 and 11 km altitude (40–60 ppbv), and on 21 June after 0600 UT between 3 and 4 km altitude (<40 ppbv). Using 3-D backward trajectory analysis with a trajectory model made available by the British Atmospheric Data Center that uses ECMWF analyzed u , v , and ω on a horizontal resolution of $2.5^\circ \times 2.5^\circ$ (see <http://www.badctrj.rl.ac.uk/>), we determined the origins of these ozone-poor air masses and their relation with the intrusion. Results for eight-day backward trajectories starting from the UT/LS on 20 June are shown in Figure 2. The ozone-poor air mostly originates from the tropical North Atlantic region (green trajectories in Figure 2), where relatively low pollution levels, strong insolation and high water vapor concentrations cause efficient ozone destruction. A relatively steep vertical ozone concentration gradient is observed between the ozone-low air and the LS immediately above. The air masses have been transported vertically adjacent for about three days, so that the steep gradient indicates relatively inefficient mixing. The trajectories (green lines) in Figure 3 indicate that the ozone-low air mass at 3–4 km altitude on 21 June originates from the lower troposphere in the subtropical North Atlantic region.

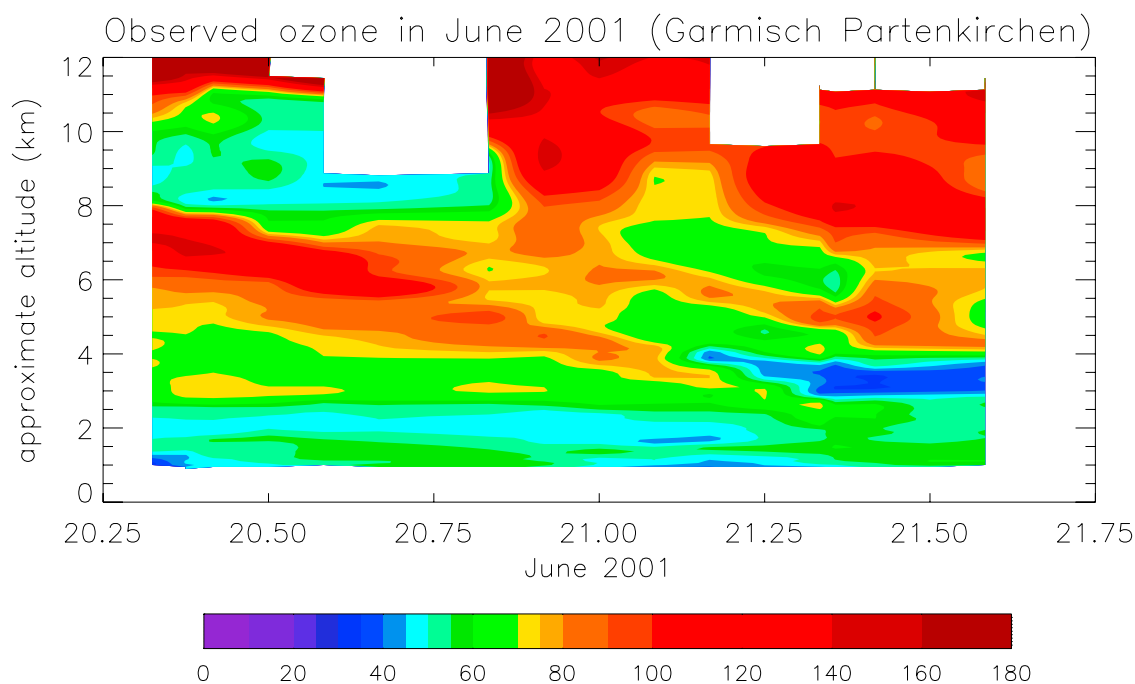


Figure 1. Lidar ozone profiles (ppbv) in Garmisch-Partenkirchen (Germany) on 20 and 21 June 2001.

[9] On 20 June between 2100 and 2400 UT a second, smaller folding event appears between 9 and 11 km altitude. This air mass is associated with a low-pressure area that moved toward Europe from the northwest in the days before. In another analysis of the same event the first intrusion event is shown as a relatively narrow region of high potential vorticity and low specific humidity that extends from northern Scandinavia to the Mediterranean region [see also *Zanis et al.*, 2003]. The second intrusion event lies between Greenland and Europe and moves eastward relatively fast. During the afternoon and evening of 20 June it collides with the first intrusion event over Europe. A smaller tongue curves toward the southwest, corresponding with the intrusion observed in the night of 20 June.

[10] On 21 June between 0600 and 1200 UT, a relatively ozone-rich feature (>90 ppbv) is observed between 4–6 km altitude. The backward trajectory analysis in Figure 3 indicates that this air mass consists of air from the North American upper and lower troposphere (blue and orange trajectories, respectively). Figure 3 illustrates the relative complexity of this event: air masses from three different origins are encountered within a 2 kilometer altitude interval. The measurements also show an ozone-rich air mass (>120 ppbv) at 7–10 km altitude that is traced back to the UT/LS over the North American east coast (trajectories not shown).

[11] We conclude that the air masses monitored in the free troposphere above Garmisch-Partenkirchen on 20–21 June originate mostly from the stratosphere and from the relatively clean marine troposphere. Consistent with this, simulated ozone production and destruction rates from the tropospheric chemistry-ECHAM model (description in section 3) indicate that ozone destruction dominates over photochemical production in these air masses.

[12] The boundary layer height is relatively constant throughout the measurement period, about 1.5 km above the surface, with typical ozone mixing ratios between

45 and 60 ppbv. Garmisch-Partenkirchen is a relatively clean Alpine location. Because of the relative coarseness of the horizontal resolution of the participating models and the complex topography in the region, the simulated chemistry in the boundary layer may not be representative of the actual conditions at the measurement site. This study will therefore not address boundary layer ozone.

3. Model Descriptions

[13] The participating models can be subdivided in three types: two chemistry-climate models, three chemistry-transport models (CTM), and one chemistry-trajectory (Lagrangian) model. The simulation of tracer advection in the models is based on analyzed meteorology from weather prediction models. The CTMs directly use the horizontal wind fields after interpolation to the model resolution, and recalculate the vertical velocities. On the other hand, the climate models simulate the actual meteorology by correcting (“nudging”) the model meteorology toward analyzed fields. The models do not include a stratospheric ozone chemistry scheme. Instead, parameterizations for stratospheric ozone based on ozone climatologies derived from observations made with ozone sondes, aircraft or satellites, or from stratospheric chemistry models, are used to represent LS ozone.

[14] The six models that participated in this exercise follow.

3.1. Tropospheric Chemistry–ECHAM (IMAU, Utrecht University, Netherlands)

[15] The tropospheric chemistry–ECHAM model combines a tropospheric chemistry module with the climate model ECHAM version 4. The horizontal resolution is T63 ($1.875^\circ \times 1.875^\circ$), the model has 19 vertical levels up to 10 hPa, and the model time step is 15 min. The

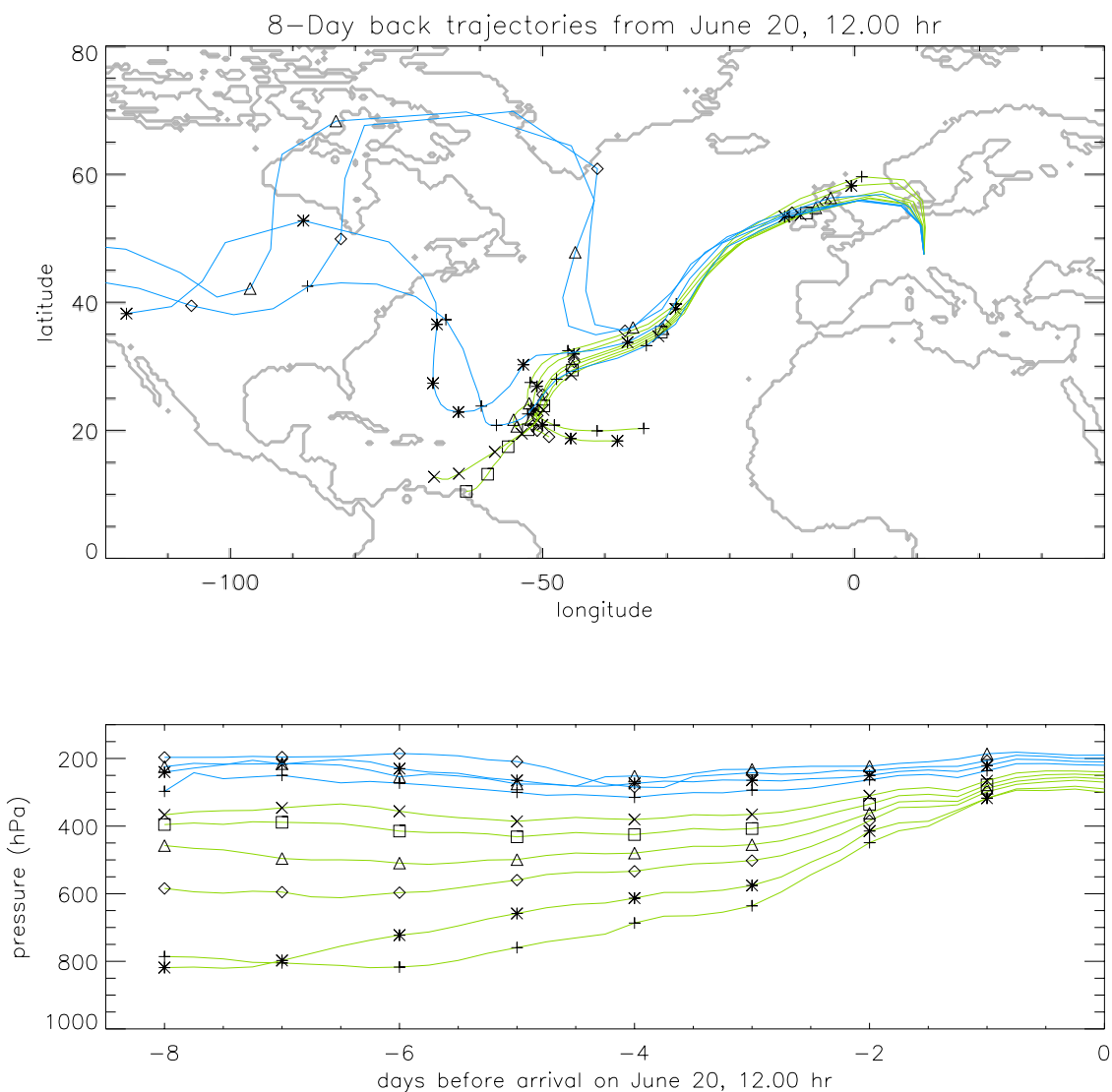


Figure 2. Eight-day backward trajectories from Garmisch-Partenkirchen starting between 8 and 12 km altitude on 20 June, 1200 UT.

meteorology is nudged with ECMWF 6-hourly spectral data for vorticity, divergence, temperature and surface pressure [Jeuken *et al.*, 1996]. Advection of tracers is calculated with a semi-Lagrangian transport scheme. The model uses a CBM4 chemistry scheme, where higher hydrocarbon species are grouped according to their functional groups and reactivity. Stratospheric ozone is parameterized with zonal and monthly averaged concentrations obtained with a 2-D stratospheric chemistry model. Additionally, the model applies an ozone-potential vorticity (PV; unit in PVU) correlation in the LS to preserve longitudinal variability due to jet stream excursions. Ozone is parameterized upward from a few layers above the tropopause (defined as the 3.5 PVU level), to allow for free mixing in the UT/LS region. A detailed model description is given by Roelofs and Lelieveld [1997] and Kentarchos *et al.* [2000].

3.2. LMDzT/INCA (LSCE, France)

[16] The LMDzT/INCA model combines a tropospheric chemistry module with the climate model LMDzT. The

horizontal resolution is $2.25^\circ \times 1.837^\circ$, the model has 50 vertical levels with about 20 levels in the troposphere, the top level of the model is 0.07 hPa, and the model time steps for dynamics, advection and chemistry/physics are 2, 10 and 30 min, respectively. The meteorology is nudged with ECMWF 6-hourly horizontal wind data. Advection of ozone is modeled using the advection scheme of Prather [1986]. For this experiment the model uses a methane oxidation chemistry scheme. Stratospheric ozone is prescribed above 380K (comparable to approximately 100 hPa in the tropics and 150 hPa in the extratropics) with a monthly ozone climatology [Li and Shine, 1995]. The stratospheric ozone parameterization was applied during the spin-up time of the simulation, but switched off after 17 June 2001. A model description is given by Jourdain and Hauglustaine [2001].

3.3. TM3 (KNMI, Netherlands)

[17] The horizontal resolution of the TM3 chemistry-transport model is $2.5^\circ \times 2.5^\circ$ for this study, the model has 31 vertical levels up to 10 hPa, and the model time step

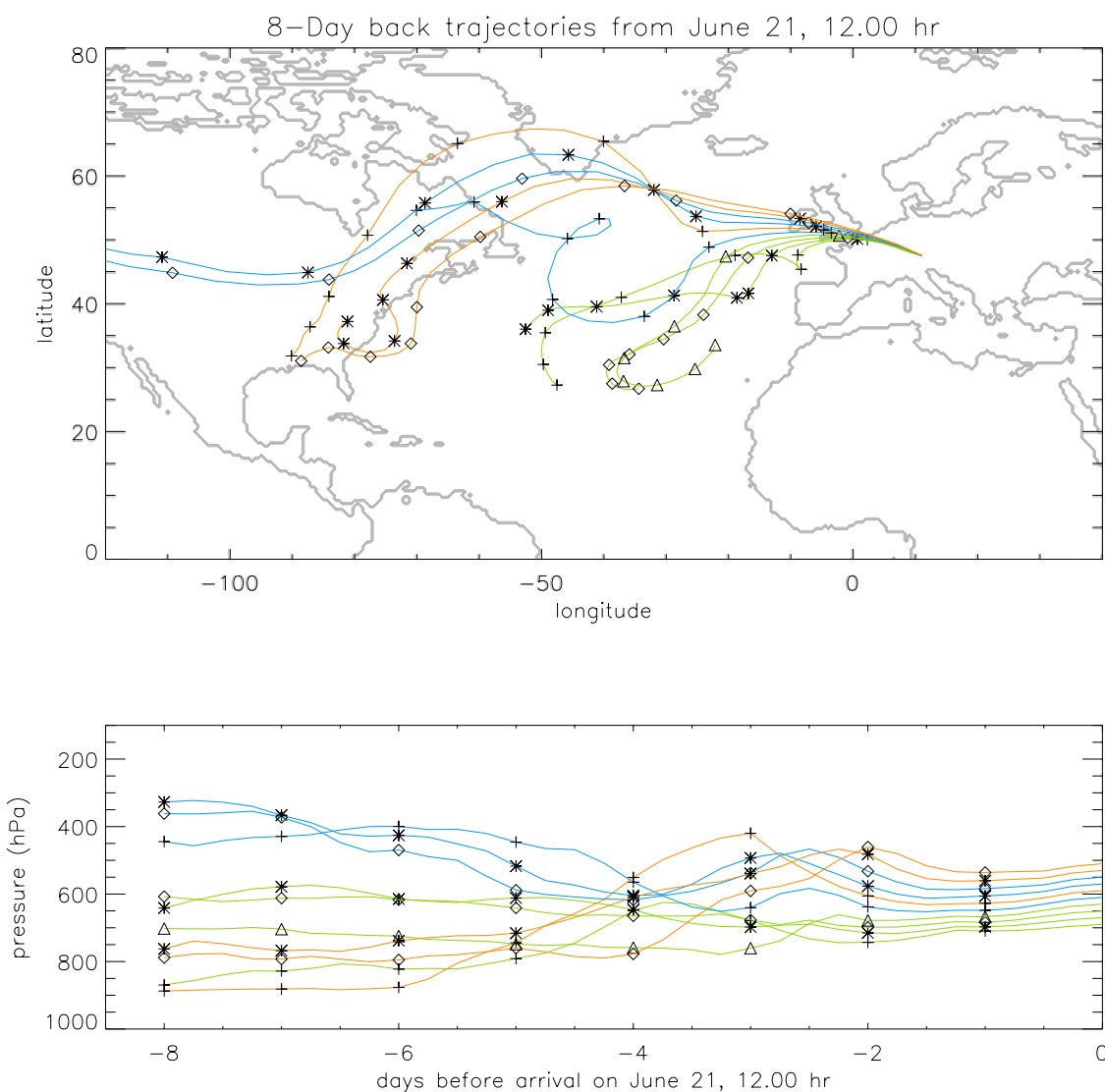


Figure 3. As in Figure 2 but for 3–5 km altitude on 21 June, 1200 UT.

is 30 min. The modeled transport is driven by ECMWF wind fields. Advection is calculated with a slopes scheme. The model uses a CBM4 chemistry scheme. Ozone is parameterized in model levels above 50 hPa with an ozone climatology derived from ozone sonde observations, and subsequent scaling toward monthly ozone columns retrieved from TOMS. A model description is given by *Jeuken et al.* [1999].

3.4. TOMCAT (University of Cambridge, UK)

[18] The horizontal resolution of the TOMCAT chemistry-transport model is T42 ($2.8^\circ \times 2.8^\circ$), the model has 31 vertical levels up to 10 hPa, and the model time step for dynamics and chemistry are 30 and 15 min, respectively. Transport in TOMCAT is driven by ECMWF meteorology obtained with a newer version of the weather prediction model that has a top level at 0.01 hPa, so it includes the complete stratosphere, and with a relatively high vertical resolution. The other models use meteorological fields with a lower level and a coarser vertical resolution. Advection is calculated with the advection scheme of *Prather* [1986]. The model uses a methane oxidation chemistry scheme

with additional reactions for ethane and propane degradation. Stratospheric ozone is specified every 5 days on the basis of results from a 2-D model that includes detailed stratospheric chemistry. Ozone is only overwritten at the top level, i.e., 10 hPa, so that LS ozone depends on ozone transport and chemistry. A model description is given by *Law et al.* [1998].

3.5. MATCH-MPIC (Max Planck Institute for Chemistry, Germany)

[19] The horizontal resolution of the MATCH-MPIC chemistry-transport model is T42 ($2.8^\circ \times 2.8^\circ$) for this study. NCEP aviation analysis 3-hourly data for horizontal wind are used to drive the model transport, with a fix for the mass-wind inconsistency problem [*Jöckel et al.*, 2001]. The model has 42 vertical levels up to 2 hPa, and a model time step of 30 min. Advection is calculated with the SPITFIRE advection scheme [*Rasch and Lawrence*, 1998]. The model uses the Mainz Isoprene Mechanism with additional hydrocarbons. Stratospheric ozone is prescribed indirectly. Modeled mean zonal ozone mixing ratios, in levels at 30 hPa or more above a climatological tropopause, are scaled to match

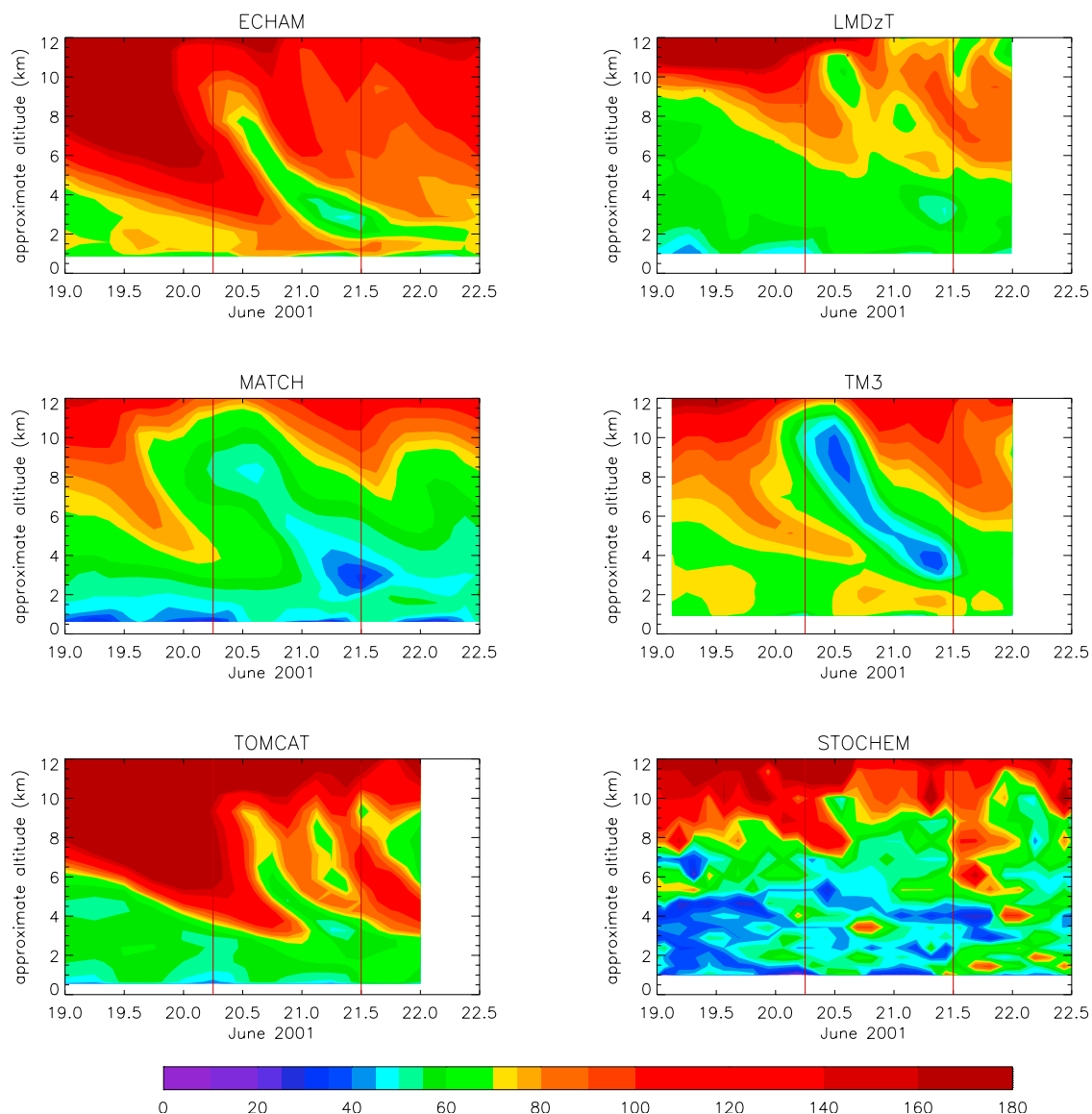


Figure 4. Simulated time-altitude ozone distributions (ppbv) for Garmisch-Partenkirchen, 20 and 21 June 2001.

zonal HALOE data so that the simulated longitudinal variability is preserved. Previous estimates of global annual STE fluxes of ozone from MATCH were rather high, ~ 1100 Tg O_3 yr $^{-1}$, and in this study STE was reduced to about 540 Tg O_3 yr $^{-1}$ by considering 50% of the stratospheric ozone amount in the advection calculations. A model description is given by Lawrence *et al.* [2002] and von Kuhlmann *et al.* [2003].

3.6. STOCHEM (Met Office, UK)

[20] STOCHEM is a parcel trajectory model, which is run coupled to the Met Office HadAM4 climate model which, for this study, is continually nudged toward ECMWF wind fields, temperature and surface pressure. The climate model has 38 levels up to a model top of 4.6 hPa, and a timestep of 30 min. Time steps for advection and chemistry are 60 and 5 min, respectively. STOCHEM subdivides the model domain in 100,000 parcels. The model uses a chemistry scheme involving oxidation of hydrocarbons up to C4 and

isoprene. Ozone concentrations above the tropopause are relaxed with a 20 day e-folding time toward the monthly ozone climatology from Li and Shine [1995]. A model description is presented by Collins *et al.* [2002].

4. Evaluation of Model Performances

4.1. Time-Height Distributions

[21] Figure 4 shows the time-altitude ozone distributions simulated by the models for 18–22 June at Garmisch-Partenkirchen. The measurement period, approximately between 20 June, 0700 UT (i.e., 20.3), and 21 June, 1200 UT (i.e., 21.5), is indicated by vertical lines.

[22] Most models clearly represent the intrusion as a mid-tropospheric, relatively ozone-rich tongue of air, comparable to that observed on 20 June (Figure 1). The results from the Lagrangian model STOCHEM, which appear irregular compared to the other models, will be discussed at the end of this section.

[23] The simulated width and depth of the intrusion and associated ozone mixing ratios vary strongly between the models. ECHAM and TOMCAT simulate ozone mixing ratios in the intrusion layer of more than 100 ppbv, which agrees with the observations. MATCH and TM3, on the other hand, simulate rather low concentrations in the intrusion, but they reproduce the ozone-poor air mass in the UT on 20 June relatively well. LMDzT/INCA also simulates this, but the simulated intrusion appears to be less deep than in other models, which is probably related to the fact that only horizontal wind components are nudged. Most models simulate an increase of UT ozone in the evening of 20 June, but only in ECHAM, TOMCAT and LMDzT/INCA does this appear as a distinctive intrusion event. The ozone minimum between 3 and 4 km altitude on 21 June is reproduced by all models, although ozone is somewhat overestimated by ECHAM, LMDzT and TOMCAT. All models simulate relatively high ozone amounts in the UT at noon on 21 June, but only TOMCAT and LMDzT/INCA reproduce the observed maximum. TOMCAT simulates more ozone than observed in the LS, which may be due to overestimated ozone amounts in the 2-D climatology used in the stratospheric ozone parameterization. MATCH and TM3 underestimate LS ozone, and therefore also in the intrusion.

[24] For the representativity of the simulated ozone distributions, the type of model, i.e., CTM or climate model, appears not to be a determinant factor. The results from TM3 and MATCH, both a CTM, emphasize the relatively ozone-low air masses during the event, whereas the results of the chemistry-climate model ECHAM and the CTM TOMCAT make air masses of stratospheric origin more prominent. The results from ECHAM and LMDzT/INCA, which are both chemistry-climate models, are considerably different. We will examine the simulated ozone profiles in more detail in section 4.2.

[25] STOCHEM is the only Lagrangian model in the intercomparison. In a Lagrangian model the atmosphere is subdivided in air parcels. While a Eulerian model calculates transport of air between grid cells, in a Lagrangian model the parcels are transported through the model domain. A concentration profile is obtained by sampling the parcels with coordinates at or near a specified time and location. Obviously, models that consider more parcels are capable of a more realistic representation of the sampled profiles. For example, the Lagrangian model FLEXPART uses 3.5 million parcels originating in the stratosphere only [Stohl and Trickl, 1999], resulting in relatively smooth tracer profiles. It appears therefore that the number of parcels used to represent the atmosphere in STOCHEM, i.e., 100,000, is insufficient to produce relatively smooth instantaneous distributions, although time-averaged, e.g., monthly or seasonal, distributions appear more representative [Collins *et al.*, 2002]. A significant increase of the parcel density in STOCHEM, e.g., by a factor of 10, is currently not feasible because of the computationally expensive chemistry calculations involved. The STOCHEM results in Figure 4 indicate the presence of the large intrusion on 20 June, while the small ozone maximum at ~ 3.5 km altitude on 20 June around 1800 UT may be associated with that same intrusion. The relatively ozone-poor parcels simulated on 21 June at 4 km altitude are also consistent with the observa-

tions and the results from the other models, as is the relatively high ozone concentration in the UT/LS before noon on 21 June.

4.2. Vertical Ozone Profiles

[26] Figure 5 compares observed and simulated ozone profiles at selected times during the measurement period.

4.2.1. Time 20 June, 1200 UT

[27] On 20 June, 1200 UT, the observations show that the ozone-rich layer associated with the main intrusion event is located between 6 and 7 km altitude. It has a thickness of 1–2 km and a peak ozone concentration of 140 ppbv. ECHAM and TOMCAT simulate similar ozone levels in the intrusion, but the layer is thicker and the altitude is lower than observed. TM3 and MATCH produce a maximum at the same altitude as ECHAM and TOMCAT but with only 70–80 ppbv ozone. LMDzT/INCA places the intrusion somewhat higher than observed and also underestimates ozone. STOCHEM simulates a local ozone maximum at 8 km altitude, also somewhat above the observed altitude of the intrusion.

[28] MATCH and TM3 reproduce the observed ozone minimum between 7–11 km altitude relatively well with concentrations of 45–55 ppbv, but they simulate a less steep ozone concentration gradient at the tropopause and generally underestimate ozone in the LS. For MATCH this is probably related to the artificial reduction of ozone transport from the middle to the lower stratosphere (see section 3). Also, MATCH and TM3 scale stratospheric ozone amounts to match time-averaged ozone distributions retrieved from satellite measurements, but this may not adequately represent the dynamically induced longitudinal variability of LS ozone levels. In ECHAM and TOMCAT the modeled ozone concentration gradient appears more realistic, especially in TOMCAT, which has a finer vertical resolution around the tropopause. A previous study with different ECHAM versions already indicated that a finer vertical resolution somewhat reduces the strength of STE and better represents a sharper concentration gradient at the tropopause [Land *et al.*, 2002]. However, both models overestimate ozone in the ozone-poor air mass by 20 to 40 ppbv. STOCHEM and LMDzT/INCA simulate an UT/LS concentration gradient comparable to the observed one.

4.2.2. Time 20 June, 2100 UT

[29] On 20 June, 2100 UT, the observed intrusion has descended to about 4 km altitude, while ozone has dropped from 140 to about 80 ppbv. TOMCAT and STOCHEM simulate the intrusion somewhat lower than the observed altitude, but they approximate observed ozone levels relatively well. It must be remarked, however, that the air parcels in STOCHEM may not fully represent the actual vertical extent and thickness of the intrusion because of the relatively coarse parcel resolution. In ECHAM the layer descends faster and deeper than observed, affecting ozone levels in the boundary layer as well. It has earlier been suggested that the combination of a relatively coarse vertical resolution and the semi-Lagrangian transport scheme make vertical transport in ECHAM relatively diffusive [Land *et al.*, 2002; Meloen *et al.*, 2003]. The upper tropospheric intrusion in the night of 20 June appears in the observations as a local ozone maximum between 8 and 10 km altitude, but this feature is generally not well resolved by the models.

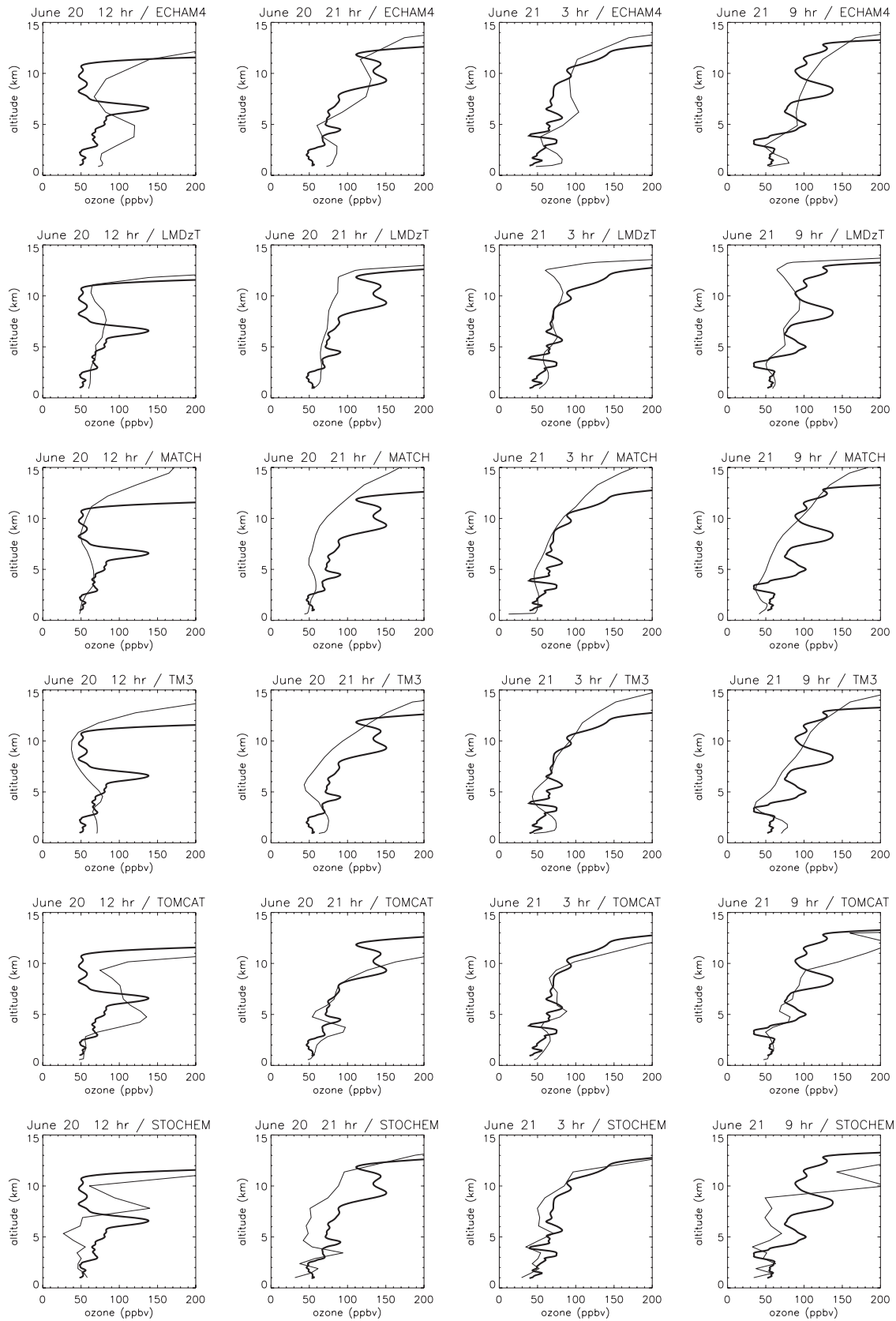


Figure 5. Observed (thick line) and simulated (thin line) ozone profiles at Garmisch-Partenkirchen.

4.2.3. Time 21 June, 0300 UT

[30] On 21 June, 0300 UT, the relatively ozone-poor layer of marine lower tropospheric origin (see section 3) is now observed at 4 km altitude. All models simulate this feature qualitatively well probably because this air mass originates from and is transported through the lower troposphere where the vertical resolution of the models is relatively fine. However, the observed concentration gradients upward and downward from the minimum are not reproduced. The ozone maximum at 6 km altitude is reproduced by TOMCAT and STOCHEM relatively well, but less successfully so by the other models. This illustrates the impact from the relatively fine vertical resolution in TOMCAT and the absence of numerical diffusion in the Lagrangian model STOCHEM on the model performance. ECHAM overestimates ozone at this altitude. MATCH and TM3 do not simulate this layer but on average their simulated ozone profiles in the free troposphere agree with the observations. LMDzT/INCA simulates an ozone minimum below the tropopause that is more pronounced than observed.

4.2.4. Time 21 June, 0900 UT

[31] Between 4 and 6 km altitude an ozone-rich air mass is observed on 21 June, 0900 UT. This is reproduced relatively well by TOMCAT and STOCHEM, and to a smaller extent by ECHAM, while it is less pronounced in the other models. The relatively ozone-rich layer between 7 and 9 km altitude is not captured by the models at this particular time, although LMDzT/INCA, TOMCAT and STOCHEM simulate a maximum at this altitude at a later instant (Figure 4). Again, the ozone-poor air mass in the lower troposphere is captured relatively well.

5. Contribution of Ozone From the Lower Stratosphere

[32] In this section we examine the contribution from ozone of stratospheric origin to ozone amounts in and near the intrusion. ECHAM results will be used for this. ECHAM includes a chemical tracer, referred to as O_{3s} , that is prescribed in the stratosphere in the same way as ozone (section 3). In the troposphere, ozone is photochemically destroyed but also produced. However, the O_{3s} tracer is photochemically destroyed but not produced. Calculation of the photochemical destruction of O_{3s} is based on the odd-oxygen family concept, with the major reactions being the photodissociation of O_3 and subsequent reaction of the $O(^1D)$ produced with water vapor yielding two OH radicals, and reaction of O_{3s} with OH or HO_2 . The difference between O_3 and O_{3s} , referred to as O_{3t} , thus reflects the photochemical production of ozone. Because the extratropical LS is generally dominated by chemical destruction of ozone, O_{3t} originates mainly from photochemical production in the troposphere. Note that O_3 and O_{3s} are also removed by dry deposition.

[33] Figure 6 shows the simulated time-altitude distribution of ozone, already presented in Figure 4, and those of O_{3s} and O_{3t} . The stratosphere contributes 70% or more to ozone in the first and second intrusions, i.e., on 20 June in the morning in the middle troposphere and in the evening in the UT. O_{3t} concentrations are relatively low here. The separate distributions of O_{3s} and O_{3t} illustrate the intricate layering of air mass origins encountered in the middle and upper tropo-

spheric air in the morning of 21 June, as previously discussed in section 2. The model simulates enhanced stratospheric contributions at 5–7 km and >10 km altitude, and an enhanced tropospheric photochemical contribution at 7–10 km altitude. The latter originates from North America, and may reflect intercontinental transport of pollution. Finally, the distribution of O_{3t} in the BL shows a daily afternoon maximum similar to the observations.

[34] The results discussed in section 4 imply that the ozone content of the lower stratosphere influences that of the intrusion. To analyze this further, we used ECHAM for a sensitivity study with varying LS ozone concentrations. By adapting the ozone-PV relationship (see section 3), prescribed ozone is changed to 50%, 75% and 150% of the values in the control simulation. The results are shown in Figure 7. They demonstrate the sensitivity of simulated tropospheric ozone profiles for ozone amounts in the LS, especially in air associated with the intrusions, specifically on 20 June at 1200 UT between 3 and 6 km, on 20 June at 2100 UT between 2 and 3 km and between 8 and 10 km, and on 21 June at 0300 UT between 5 and 7 km. In the first of these air masses the calculated concentration of O_{3s} maximizes at 92 ppbv, contributing about 70–80% of the ozone in the intrusion air. In the three sensitivity studies the O_{3s} contributions are 39, 68, and 141 ppbv, respectively, which is 43, 74 and 153% of O_{3s} in the control simulation. The simulated response of O_{3s} in the intrusion is therefore almost linear with respect to LS ozone, indicating the importance of an accurate representation of ozone in the LS in tropospheric ozone models. We note that the linearity is somewhat less in the second intrusion, with O_{3s} values of 40, 70 and 160% compared to the control simulation, because of the influence of the LS ozone abundance on photochemistry in the troposphere. O_{3t} profiles are not significantly affected by this except in the 50% and 75% sensitivity simulations in which photochemical ozone production is enhanced in the boundary layer.

[35] Around noon on 20 June, the air in the upper troposphere originates from the tropical lower troposphere (Figure 2). We note that the computed O_{3t} in this air mass is of the same magnitude as observed ozone (Figure 6). The sensitivity study indicates that this ozone-poor feature is represented more realistically in the 50% and 75% simulations, although LS ozone is then underestimated. Hence the overestimation of ozone in this air mass in the ECHAM control run appears to be associated with the contribution from the stratosphere, probably because of too strong downward diffusion across the steep ozone concentration gradient at the tropopause. The qualitative similarity between simulated ozone in the UT/LS for the 50% and 75% sensitivity simulations and the results from MATCH and TM3 suggests that these models may display a similar performance.

6. Discussion and Conclusions

[36] We have compared simulation results from six tropospheric chemistry models with observed ozone profiles in Garmisch-Partenkirchen (Germany) for 20–21 June 2001. This is the first model intercomparison study that examines simulations of cross-tropopause and tropospheric transport of ozone for a specific synoptic event. The case study focuses on the representation of a relatively complex

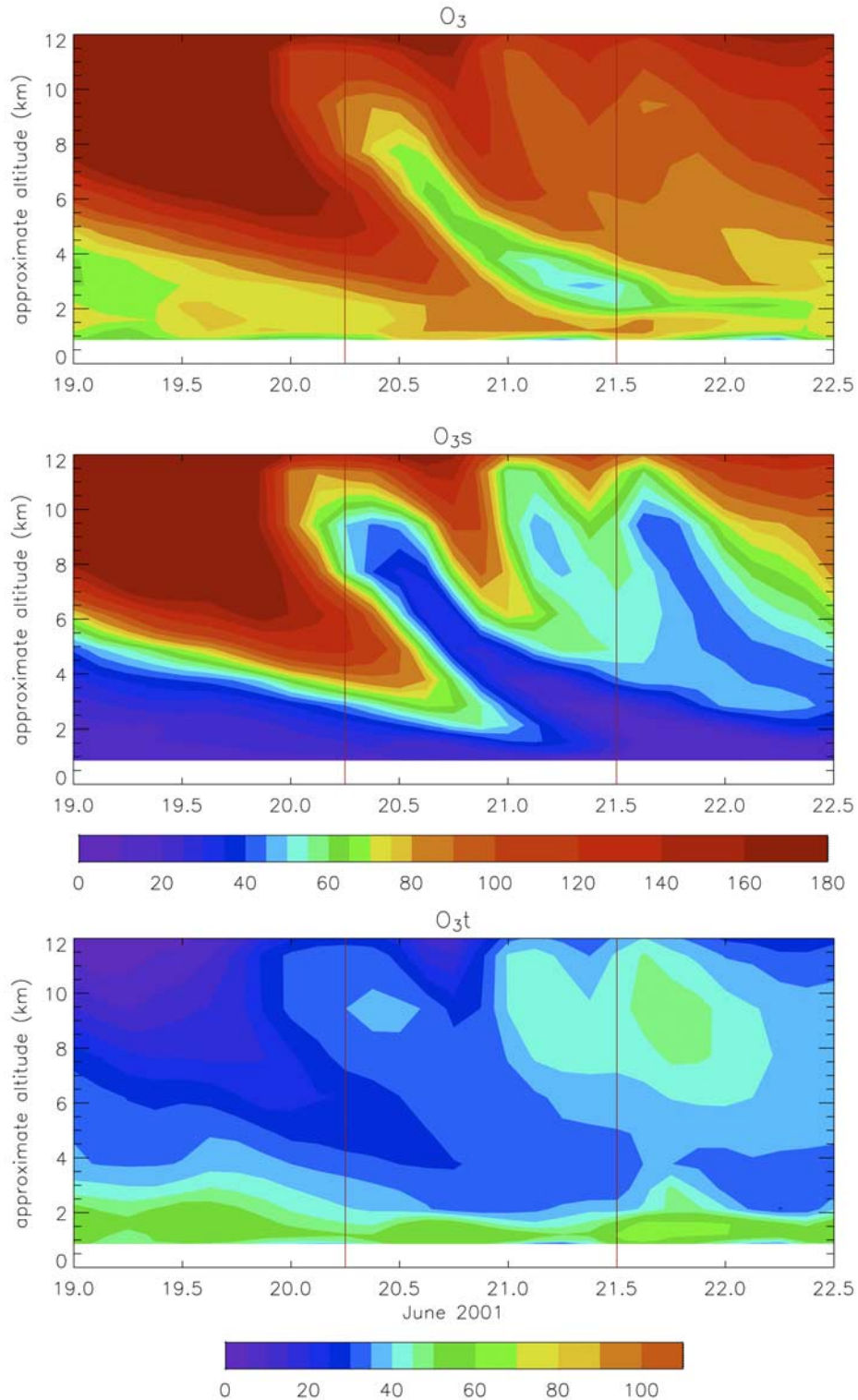


Figure 6. Time-altitude distributions for ozone (ppbv), and ozone of stratospheric (O_3s) and tropospheric (O_3t) origin for Garmisch-Partenkirchen, 20 and 21 June 2001 as simulated by ECHAM. Note the different color scale for O_3t .

synoptic disturbance that involves a number of chemically different air masses, specifically two intrusions of air of stratospheric origin and several tropospheric air masses advected by the warm and cold conveyor belts.

[37] Two coupled chemistry-climate models (ECHAM, LMDzT/INCA), three chemistry-transport models (MATCH, TM3, TOMCAT), and one chemistry-trajectory model (STOCHEM) participate. The tropospheric chemistry

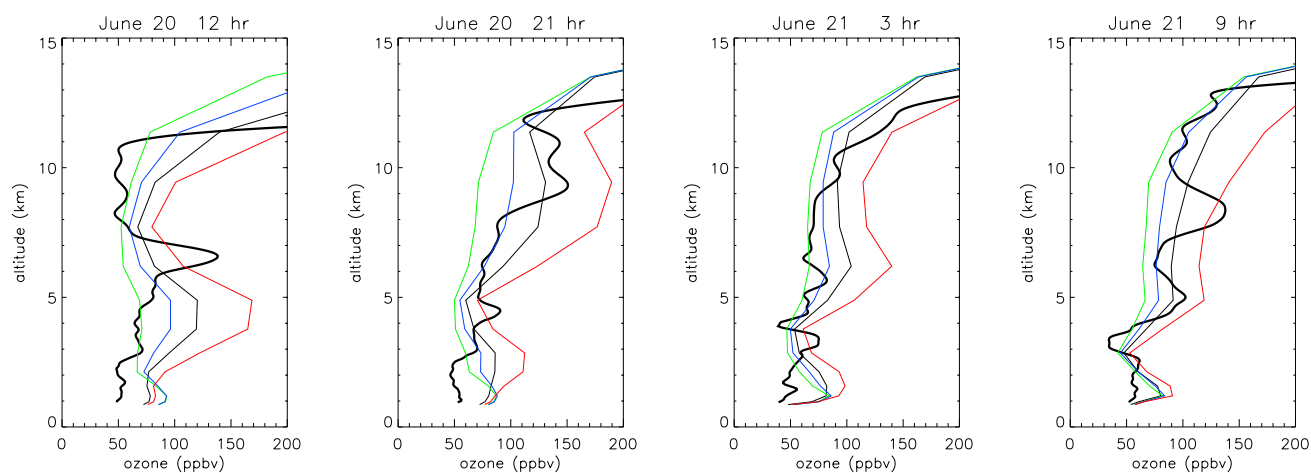


Figure 7. Observed (thick line) and simulated ozone profiles at Garmisch-Partenkirchen as simulated by ECHAM for different ozone amounts in the lower stratosphere. Black: standard simulation; green: LS ozone at 50%; blue: at 75%; red: at 150%.

models apply parameterizations that prescribe ozone mixing ratios in most of the model stratosphere (ECHAM), upward from 30 hPa above the model tropopause (MATCH), or above specific pressure levels in the model stratosphere (TM3: 50 hPa; STOCHEM: 100 hPa; LMDzT/INCA: 100–150 hPa; TOMCAT: 10 hPa). Most of the models were involved in previous intercomparisons that focused on ozone climatologies [e.g., Kanakidou *et al.*, 1998; Law *et al.*, 2000].

[38] The simulation of tracer transport in the models is based on analyzed meteorological fields. All models simulate an intrusion from the stratosphere at the same time as observed, indicating that the meteorological data used by the models are consistent. Nevertheless, simulated ozone distributions differ considerably between models. We note that the intercomparison by Meloen *et al.* [2003] reveals that the vertical velocities simulated by different models, of which three partake in this intercomparison, are relatively similar. This may indicate that differences in the processing of the ECMWF meteorological data to drive model transport are probably not a major cause of the differences between the simulated ozone distributions in the troposphere for the event in our study. This processing generally consists of the interpolation of the ECMWF or NCEP wind fields to the horizontal and vertical resolution of the chemistry model, and subsequent calculation of the vertical velocities. The type of model (i.e., CTM in which transport is prescribed by the ECMWF meteorology vs. climate model in which the calculated meteorology is nudged toward the ECMWF meteorology) appears not to be important for the representativity of the simulated ozone distribution. Because most of the sampled air originates from the stratosphere or from the relatively clean sub-tropical Atlantic Ocean, ozone destruction dominates photochemical production in the free troposphere during the event, with destruction rates up to a few ppbv day⁻¹. Therefore discrepancies between simulated and observed ozone distributions are probably also not related to differences in the chemistry schemes.

[39] Backward trajectories show that air in the intrusion originates from the LS. Ozone levels in the intrusion

therefore strongly depend on ozone levels in the LS. TM3 and MATCH underestimate these, which may be due to their parameterizations for stratospheric ozone. As a result, TM3 and MATCH underestimate ozone in tropospheric air masses associated with STE, whereas background ozone levels are simulated realistically. We cannot, however, exclude the possibility that the analyzed meteorological fields contain inaccuracies, which impact downward transport between the middle and the lower stratosphere in the chemistry models. Simulated transport in the stratosphere may improve when the models that generate the meteorological data, more realistically represent the large-scale circulation by taking into account the full middle atmosphere, and apply a relatively fine vertical resolution in the UT/LS region. It appears that TOMCAT, which applies such data from ECMWF, simulates a more efficient downward transport in the stratosphere than TM3 and MATCH.

[40] ECHAM prescribes ozone almost throughout the model stratosphere so that inaccuracies in downward transport within the stratosphere do not play a large role. Instead, transport between the LS and the troposphere is of major importance for the model representativity. Because of a relatively coarse model resolution and a diffusive tracer transport scheme, ECHAM appears to overestimate diffusion across steep concentration gradients so that STE of ozone appears stronger than observed. TOMCAT simulates a more realistic evolution of the event with relatively more detail in the tropospheric ozone profiles. This is due to the relatively fine vertical resolution of the model, which suppresses diffusion. In LMDzT/INCA the ozone-rich intrusion is not very pronounced, probably because of the fact that the model is nudged toward ECMWF horizontal wind fields only. Nudging of the vorticity, instead, may improve the representation of the vertical winds. Generally, however, the order of magnitude of ozone concentrations is similar to that observed in this case study and the model appears capable of representing relatively steep concentration gradients. The Lagrangian model STOCHEM generally displays a satisfactory vertical gradient in the simulated ozone profiles, although its representativity may be enhanced by a higher parcel trajectory density.

[41] Can the results from this study help evaluate simulated global and annual cross-tropopause ozone transport budgets? The ozone profiles provide insufficient information to estimate the cross-tropopause flux of ozone for this particular event. Comparison of Figures 1 and 4 shows that the ozone mixing ratio in the intruding air is larger than observed for TOMCAT, smaller than observed for MATCH, TM3 and LMDzT/INCA, and of comparable magnitude for ECHAM and STOCHEM. Assuming that the relative strength of STE of ozone is reflected by the ozone content of the simulated intrusions, the ozone STE budget associated with this event is largest in TOMCAT and smallest in MATCH, TM3 and LMDzT/INCA. On annual and global scales, however, simulated cross-tropopause ozone fluxes are ranked differently among the models, with 459 Tg O₃ yr⁻¹ for ECHAM [Kentarchos et al., 2000], between 500 and 600 Tg O₃ yr⁻¹ for MATCH [von Kuhlmann, 2001] (available at <http://www.mpch-mainz.mpg.de/~kuhlmann>), and 565 Tg O₃ yr⁻¹ for TM3 [Lelieveld and Dentener, 2000]. This indicates that other dynamical and numerical factors contribute significantly to the simulated annual STE budget for ozone, such as large-scale advection, diffusion and numerical mixing along isentropic surfaces. More detailed understanding of the contribution of different mechanisms to the total cross-tropopause transport of air and ozone, for example, based on multiyear reanalyzed meteorological data [e.g., Sprenger and Wernli, 2003], is needed to evaluate all aspects associated with the influence of STE of ozone on the tropospheric chemical composition.

[42] We conclude that accurate simulation of tracer distributions and transport in a specific synoptic event, more specifically steep concentration gradients at the tropopause and upward and downward of the intrusion, is difficult for the present generation of tropospheric ozone models. This case study of an STE event at extra-tropical latitudes shows that an accurate representation of the ozone distribution in the lower stratosphere, consistent with the tropopause dynamics, is conditional for an accurate simulation of downward cross-tropopause ozone transport.

[43] **Acknowledgments.** The contribution of IMAU to this study is funded by the EU project STACCATO (EVK2-1999-00316). G.R. and A.K. wish to acknowledge the Dutch computer center SARA (Amsterdam) for use of computer resources and the British Atmospheric Data Center for use of their trajectory model. The contributions by Cambridge University and LSCE are partly funded by the EU projects MOZAIC III (EVK2-1999-00141) and TRADE-OFF (EVK2-CT-1999-0030), respectively. The contribution of the Met Office is partly funded by the Government Meteorological Research Program.

References

- Appenzeller, C., J. R. Holton, and K. H. Rosenlof, Seasonal variation of mass transport across the tropopause, *J. Geophys. Res.*, *101*, 15,071–15,078, 1996.
- Bregman, A., M. Krol, H. Teyssedre, W. Norton, M. Chipperfield, G. Pitari, J. Sundet, and J. Lelieveld, Chemistry-transport model comparison with ozone observations in the midlatitude lowermost stratosphere, *J. Geophys. Res.*, *106*, 17,479–17,496, 2001.
- Collins, W. J., G. R. Derwent, C. E. Johnson, and D. S. Stevenson, A comparison of two schemes for the convective transport of chemical species in a Lagrangian global chemistry model, *Q.J.R. Meteorol. Soc.*, *128*, 991–1009, 2002.
- Cooper, O. R., J. L. Moody, D. D. Parrish, M. Trainer, T. B. Reyrson, J. S. Holloway, G. Hübler, F. C. Fehsenfeld, S. J. Oltmans, and M. J. Evans, Trace gas signatures of the airstreams within North Atlantic cyclones: Case studies from the North Atlantic Regional Experiment (NARE '97) aircraft intensive, *J. Geophys. Res.*, *106*, 5437–5456, 2001.
- Cristofanelli, P., et al., Stratosphere-to-troposphere transport: A model and method evaluation, *J. Geophys. Res.*, *108*(D12), 8525, doi:10.1029/2002JD002600, 2003.
- Davies, T. D., and E. Schüpbach, Episodes of high ozone concentrations at the Earth's surface resulting from transport down from the upper troposphere/lower stratosphere: A review and case studies, *Atmos. Environ.*, *28*, 53–68, 1994.
- Eisele, H., H. E. Scheel, R. Sladkovic, and T. Trickl, High resolution lidar measurements of stratosphere-troposphere exchange, *J. Atmos. Sci.*, *56*, 319–330, 1999.
- Fehsenfeld, F. C., P. Daum, W. R. Leaitch, M. Trainer, D. D. Parrish, and G. Hübler, Transport and processing of O₃ and O₃ precursors over the North Atlantic: An overview of the 1993 North Atlantic Regional Experiment (NARE) summer intensive, *J. Geophys. Res.*, *101*, 28,877–28,891, 1996.
- Holton, J. R., P. H. Haynes, M. E. McIntyre, A. R. Douglas, R. B. Rood, and L. Pfister, Stratosphere-troposphere exchange, *Rev. Geophys.*, *33*, 403–439, 1995.
- Jacob, D. J., J. A. Logan, and P. P. Murti, Effect of rising Asian emissions on surface ozone in the United States, *Geophys. Res. Lett.*, *26*, 2175–2178, 1999.
- Jeuken, A. B. M., P. C. Siegmund, L. C. Heijboer, J. Feichter, and L. Bengtsson, On the potential of assimilating meteorological analyses in a global climate model for the purpose of model validation, *J. Geophys. Res.*, *101*, 16,939–16,950, 1996.
- Jeuken, A. B. M., H. J. Eskes, P. F. J. van Velthoven, H. M. Kelder, and E. V. Hölm, Assimilation of total ozone satellite measurements in a three-dimensional tracer transport model, *J. Geophys. Res.*, *104*, 5551–5563, 1999.
- Jöckel, P., R. von Kuhlmann, M. G. Lawrence, B. Steil, C. A. M. Brenninkmeijer, P. J. Crutzen, P. J. Rasch, and B. Eaton, On a fundamental problem in implementing flux-form advection schemes for tracer transport in 3-dimensional general circulation and chemistry transport models, *Q. J. R. Meteorol. Soc.*, *127*, 1035–1052, 2001.
- Jourdain, L., and D. Hauglustaine, The global distribution of lightning NO_x simulated on line in a general circulation model, *Phys. Chem. Earth, Part C: Sol.-Terr. Planet. Sci.*, *26*, 585–591, 2001.
- Kanakidou, M., et al., 3D global simulations of tropospheric chemistry with focus on ozone distributions: Results from the GIM/IGAC intercomparison exercise, *Rep. EUR 18842*, pp. 1–79, Eur. Comm., Brussels, 1998.
- Kentarchos, A. S., G. J. Roelofs, and J. Lelieveld, Simulation of extratropical synoptic scale stratosphere-troposphere exchange using a coupled chemistry-GCM: Sensitivity to horizontal resolution, *J. Atmos. Sci.*, *57*, 2824–2838, 2000.
- Land, C., J. Feichter, and R. Sausen, Impact of vertical resolution on the transport of passive tracers in the ECHAM4 model, *Tellus, Ser. B*, *54*, 344–360, 2002.
- Law, K. S., P. H. Plantevin, D. E. Shallcross, H. L. Rogers, J. A. Pyle, C. Grouhel, V. Thouret, and A. Marengo, Evaluation of modeled O₃ using Measurement of Ozone and Water Vapor by Airbus In-Service Aircraft (MOZAIC) data, *J. Geophys. Res.*, *103*, 25,721–25,737, 1998.
- Law, K. S., P.-H. Plantevin, V. Thouret, A. Marengo, W. A. H. Asman, M. G. Lawrence, P. J. Crutzen, J.-F. Müller, D. A. Hauglustaine, and M. Kanakidou, Comparison between global chemistry transport model results and Measurement of Ozone and Water Vapor by Airbus In-Service Aircraft (MOZAIC) data, *J. Geophys. Res.*, *105*, 1503–1525, 2000.
- Lawrence, M. G., et al., Global chemical weather forecasts for field campaign planning: Predictions and observations of large-scale features during MINOS, CONTRACE and INDOEX, *Atmos. Chem. Phys. Discuss.*, *2*, 1545–1597, 2002.
- Lelieveld, J., and F. J. Dentener, What controls tropospheric ozone?, *J. Geophys. Res.*, *105*, 3531–3551, 2000.
- Lelieveld, J., et al., Tropospheric ozone and related processes, in *Scientific Assessment of Ozone Depletion: 1998*, *Rep. 44*, pp. 8.1–8.42, World Meteorol. Organ., Geneva, 1999.
- Lelieveld, J., et al., Global air pollution crossroads over the Mediterranean, *Science*, *298*, 794–799, 2002.
- Levy, H., II, Normal atmosphere: Large radical and formaldehyde concentrations predicted, *Science*, *173*, 141–143, 1971.
- Li, D., and K. P. Shine, A 4-dimensional ozone climatology for UGAMP models, UGAMP internal report 35, UK Univ. Gloal Atmos. Model. Programme, Cent. of Atmos. Sci., Univ. of Cambridge, Cambridge, UK, 1995.
- Meloan, J., et al., Stratosphere-troposphere exchange: A model and method intercomparison, *J. Geophys. Res.*, *108*(D12), 8526, doi:10.1029/2002JD002274, 2003.
- Prather, M. J., Numerical advection by conservation of second-order moments, *J. Geophys. Res.*, *91*, 6671–6681d, 1986.
- Prather, M. J., et al., Atmospheric chemistry and greenhouse gases, in *Climate Change 2001: The Scientific Basis, Contribution of Working Group I to the Third Assessment Report of the Intergovernmental Panel*

- on *Climate Change*, edited by J. T. Houghton et al., pp. 239–287, Cambridge Univ. Press, New York, 2001.
- Ramanathan, V., et al., Climate-chemical interactions and effects of changing atmospheric trace gases, *Rev. Geophys.*, 25, 1441–1482, 1987.
- Rasch, P. J., and M. G. Lawrence, Recent developments in transport methods at NCAR, in *MPI Workshop on Conservative Transport Schemes*, pp. 65–75, Max Planck Inst. for Meteorol., Hamburg, Germany, 1998.
- Roelofs, G. J., and J. Lelieveld, Model study of the influence of cross-tropopause O₃ transports on tropospheric O₃ levels, *Tellus, Ser. B*, 49, 38–55, 1997.
- Roelofs, G. J., H. A. Scheeren, J. Heland, H. Ziereis, and J. Lelieveld, A model study of ozone in the eastern Mediterranean free troposphere during MINOS (August 2001), *Atmos. Chem. Phys. Discuss.*, 3, 1247–1272, 2003.
- Sprenger, M., and H. Wernli, A northern hemispheric climatology of cross-tropopause exchange for the ERA15 time period (1979–1993), *J. Geophys. Res.*, 108(D12), 8521, doi:10.1029/2002JD002636, 2003.
- Stohl, A., and T. Trickl, A textbook example of long-range transport: Simultaneous observation of ozone maxima of stratospheric and North American origin in the free troposphere over Europe, *J. Geophys. Res.*, 104, 30,445–30,462, 1999.
- Stohl, A., et al., Stratosphere-troposphere exchange: A review, and what we have learned from STACCATO, *J. Geophys. Res.*, 108(D12), 8516, doi:10.1029/2002JD002490, 2003.
- Trickl, T., O. C. Cooper, H. Eisele, P. James, R. Mücke, and A. Stohl, Intercontinental transport and its influence on the ozone concentrations over central Europe: Three case studies, *J. Geophys. Res.*, 108, doi:10.1029/2002JD002735, in press, 2003.
- Vaughan, G., Stratosphere-troposphere exchange of ozone, in *Tropospheric Ozone*, edited by I. S. A. Isaksen, pp. 125–135, D. Reidel, Norwell, Mass., 1988.
- von Kuhlmann, R., Tropospheric photochemistry of ozone, its precursors and the hydroxyl radical: A 3D-modeling study considering non-methane hydrocarbons, Ph.D. thesis, Univ. of Mainz, Mainz, Germany, 2001.
- von Kuhlmann, R., M. G. Lawrence, P. J. Crutzen, and P. J. Rasch, A model for studies of tropospheric ozone and non-methane hydrocarbons: Model description and ozone results, *J. Geophys. Res.*, 108(D9), 4294, doi:10.1029/2002JD002893, 2003.
- Zanis, P., et al., Forecast, observation and modelling of a deep stratospheric intrusion event over Europe, *Atmos. Chem. Phys. Discuss.*, 3, 1109–1138, 2003.
-
- W. J. Collins, Climate Research Division, Met Office, London Road, Bracknell, Berkshire RG5 3AD, UK.
- R. A. Crowther and K. S. Law, Centre for Atmospheric Science, University of Cambridge, Lensfield Road, Cambridge CB2 1EW, UK.
- D. Hauglustaine and A. Klonecki, Laboratoire des Sciences du Climat et de L'Environnement, L'Orme des Merisiers, Bat. 709, F-91191 Gif-sur Yvette Cedex, France.
- A. S. Kentarchos, Environmental Research & Services (ERS-Srl), c/o European Economic Interest Group–GEOPHYSICA, Via Pancaldo 21, 50127 Firenze, Italy.
- G. J. Roelofs, Institute for Marine and Atmospheric Research Utrecht, Utrecht University, P. O. Box 8005, NL-35008 TA Utrecht, Netherlands. (g.j.roelofs@phys.uu.nl)
- A. Stohl, Department of Ecology, Technical University Munich, Am Hochanger 13, D-85354 Freising-Weihenstephan, Germany.
- T. Trickl, Institut für Meteorologie und Klimaforschung, Forschungszentrum Karlsruhe, Kreuzeckbahnstraße 19, D-82467 Garmisch-Partenkirchen, Germany.
- M. van Weele, Royal Netherlands Meteorological Institute, Wilhelminalaan 10, P. O. Box 201, NL-3730 AE De Bilt, Netherlands.
- R. von Kuhlmann and M. G. Lawrence, Max Planck Institute for Chemistry, Becherweg 27, D-55128 Mainz, Germany.